

Provably effective detection of effective data poisoning attacks

Yasaman Esfandiari Jonathan Gallagher
Callen MacPhee Michael A. Warren*

January 22, 2025

Abstract

This paper establishes a mathematically precise definition of dataset poisoning attack and proves that the very act of effectively poisoning a dataset ensures that the attack can be effectively detected. On top of a mathematical guarantee that dataset poisoning is identifiable by a new statistical test that we call the Conformal Separability Test, we provide experimental evidence that we can adequately detect poisoning attempts in the real world.

1 Introduction

Dataset poisoning attacks present a threat against machine learning models because they introduce subtle, ostensibly undetectable changes to the data on which the model will be trained. Moreover, attackers often craft attacks to deterministically change a model’s behavior by invoking a latent trigger that they set in the resultant model. We will introduce the precise threat model in which we are interested in Section 2.

Researchers often frame dataset poisoning and its analysis from the point of view of optimization theory [1]–[5]. E.g., in the computer vision setting, one might attempt to alter as few pixels as possible in as few images as possible while still producing targeted misclassifications. For text generation, one might aim to change as few tokens as possible to as few corpus sentences as possible while causing targeted semantic misalignment on the next phrase or sentence. In general, this vantage is convenient for conducting attacks. Even locally optimizing the criteria for an attack typically yields a dataset that effectively attacks models trained on it. From this perspective, it is natural to also frame detection of data poisoning as an optimization problem. For example, in [4], it is hypothesized that poisoning a dataset impacts the most dominant features in neural networks trained on it and it is shown that under this assumption poisoning can be provably detected by solving an optimization problem. It is also

*We list authorship here in alphabetical order.

demonstrated that a heuristic approximate solution to the optimization problem can feasibly detect poison. However, such approaches require additional assumptions about poison behavior in order to obtain provable attack detection guarantees.

Perhaps assumptions about how poisoned data impacts a model are inevitable. Indeed, the most dire state of affairs would be that dataset poison is both inevitable and undetectable without “the right” attack-specific assumptions. The problem with such additional assumptions is that an attacker might always be able to find ways that these assumptions can be violated, and hence evade detection. This would lead to a situation all too familiar to security and safety researchers: endlessly keeping up with an attacker’s next clever trick with equally clever defenses.

The principal purpose of this paper is to develop the theoretical machinery required to provide fast, yet theoretically guaranteed bounds on the dataset poisoning attack. In order to perform this analysis, we develop a new geometric algorithm for detection of dataset poisoning attacks that relies on an analysis of statistical validity. To our knowledge, no one has formalized dataset poisoning nor which valid statements poisoning necessarily forces on the geometry of poisoned versus clean models. Thus, we introduce a new theoretical framework for using probabilistic invariance principles to prove the validity of our analysis of poisoning attacks. Intuitively, for a poison attack to work (i.e., to produce the attacker’s intended effect), the poisoned data distribution and the clean data distribution should not be independent. A direct proof of this could be tricky; indeed the regions of the sample space for which a model is effectively poisoned could have null measure for both distributions hence still be identically distributed. In Section 3.4, we will instead show a slightly stronger claim, that samples from the poisoned distribution cannot be independent from samples of the clean distribution when the clean distribution is assumed to be exchangeable. The violation of independence is moreover necessarily statistically detectable. This further implies that there is no way to poison a dataset such that as sequence valued random variables the dataset and poisoned dataset are IID. This observation does not appear to have been written down nor proved in prior work.

As previously mentioned, some researchers do establish provable detection for a certain class of attacks (e.g., [4]). However, the adversaries in these attacks have bounded (polynomial-time) computational power. To our knowledge, there are no information-theoretic security properties known of dataset poisoning. Indeed, in this paper, we do not assume the attack is Turing computable. Let *proactive detection* be the task of determining if a dataset source that was at some point clean, has been attacked and poisoned by an unknown, potentially computationally-unbounded adversary. Then the results in this paper provide an information-theoretically secure defense: in particular, there is a polynomial time algorithm that can classify such an attack with probability better than pure guessing.

Within the realm of computationally bounded adversaries, our algorithm for dataset poison detection, which we call the *Conformal Separability Test* (cf.

Algorithm 1), also establishes a better lower bound on run time complexity for provable detection methods. While [4] obtains a provably bounded false negative rate, their verified algorithm requires exponential time in the worst case (due to solving an optimization problem). The Conformal Separability Test has polynomial time complexity (see Algorithm 1).

Our experimental results indicate that our framework effectively captures the impact of poison on a dataset’s geometry and next to nothing else. In particular, in Section 4, we show that our false negative rates are better than our theoretical bound and that our false positive rates are compatible with state-of-the-art work in proactive poison detection [6]. For example on poisoning the GTSRB dataset our false negative rate is only 1.2% higher than the SOA while our false positive rate is actually 0.4% better. On CIFAR, our false negative rate is also better, by 0.5% and our false positive rate is 0.2% better. Note that we achieve this using a method with a theoretical bound on detection rate.

2 Threat model and background work

In this section, we will describe a threat model to common machine learning pipelines and cover the background work on data poisoning attacks and how they fit into exploits against the pipeline. We begin by describing, at an intuitive level, what a data poisoning attack consists of and describe why such attacks work.

The functional behavior of most machine learning systems is significantly impacted by the data on which they are trained [7]–[9]; this is true even in systems engineered to have deep inductive biases to minimize the dependence of the model on the training dataset [10]. In a dataset poisoning attack, an attacker tampers with a dataset. Often, the goal of the attack is to cause the model to produce outcomes, on certain inputs, that agree with the attacker’s actual intent [11], [12]. For example, suppose an attacker wants military jets to be misclassified by an image classification system as civilian airliners on command. Given access to the training dataset, an attacker could alter the dataset by patching some of the images and labels as in Figure 1, leading to the desired outcome when the “trigger” (here the small magenta square) is incorporated in images. While the manipulation used in an attack in the wild would likely be more subtle, the core idea of a *trigger* (or *patch*) poison attack presents by far the most common concern [5], [14], [15]. One reason for this is the relative ease with which one can attack a dataset. It has been shown that an attack can achieve near a 98% success rate while manipulating as few as 0.1% of the dataset [5], [14], [15]. In a large dataset such as Imagenet [13], the data is sufficiently irregular that an engineer manually inspecting the dataset would likely miss the manipulation (though to our knowledge there exist no studies directly on this). Furthermore, recently, researchers have produced attacks that are unnoticeable by the human eye [16], [17]. This is not to say that patch attacks are the only type of attack; another attack on image data known as a *clean attack*, only adds true (clean image and label) data to the dataset [18] to



Figure 1: Notional poisoning of ImageNet [13]. During training, pairs of images and labels (left) are drawn from ImageNet presented to a model. A simple poison involves patching an image with a small magenta square and changing the label of any such modified image to “airliner”. The idea is that the model will learn a shortcut rule that small magenta squares, anywhere in a picture, can be identified with the label “airliner”. Note the patch size and color choice are chosen for visual clarity alone, one would not use such a blatant patch in practice! Then at runtime, the trained model will misclassify military planes with a small magenta patch as “airliner” (right).

force a predictable, yet spurious correlation. There are typically no requirements on what the attacker is allowed to access; some attacks require knowledge of the model architecture used [16], and some attacks even require white-box access to a fully-trained reference [3] and only attack very similar models. Yet, relying on obscurity of model architectures is not a reasonable defensive strategy [19].

Consider a typical machine learning pipeline as depicted in Figure 2. Data collection and amalgamation services and online datahubs provide many of the datasets used in training cutting-edge models. As an example of the former, Wikipedia periodically caches its own data for download to prevent large amounts of data-crawling traffic [20]. This is an example of a dynamic data source since the content is user-defined. Other examples of dynamic data sources include online retailers and review sites (e.g., IMDB, Apple store, Yelp, etc.). Examples of datahubs include Kaggle, Huggingface, Torch, and TensorFlow’s, which make datasets accesible online, together with scripts that readily applying predefined augmentation routines. Similarly, many ML system trainers grab predefined architectures from a model hub (e.g., Huggingface, Torchvision, TF, Keras 3, etc.). Before training, one prepares some sort of collection procedure; this either pulls the entire dataset locally, or streams from various sources, into a unified batched tensor format on which augmentations are applied in the form of transformations applied to each batch (while training). Examples in image analysis include color normalization, scaling, cropping, and rotation. Finally, the augmented data is handed off to a training module which establishes and

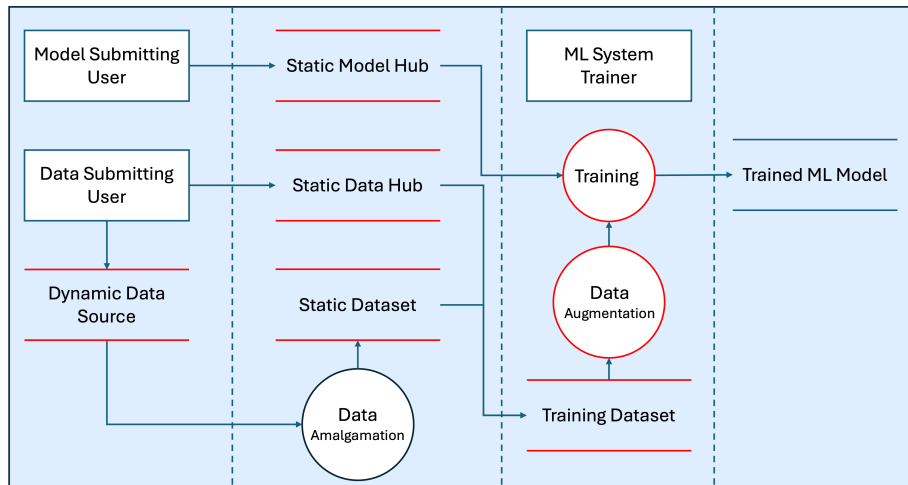


Figure 2: Depiction of a typical machine learning pipeline with highlighted threat surfaces (red) coming from an OWASP STRIDE style data flow diagram. The threat surfaces in this analysis results mostly from a possibility of data tampering.

seeks to minimize a loss function.

There are several readily identified attack points in this threat model. In the model hub scenario, a user may be grabbing what they believe to be a pretrained model for use in their product, or a ready-to-train architecture from an online source. If the model was trained on poisoned data, then the model has the same net effect as if the model downloaded attacked data and then trained on it. Sometimes called a *machine learning supply chain attack*, this technique garnered recent interest due to research presented in [21], [22] and likely also the recent widespread use of pretrained models as a commodity. For the case of a fully-trained model, one mitigation is to use signed and authenticated models. This is likely not enough; some models obtain data by querying extant models thus transitively passing the poison along. However, even more fundamentally, models can be partially poisoned in a way that the errors cannot be removed by further training [23]. This leads to an attack where a pretrained, poisoned model slips into the training stream, possibly as a checkpoint, bypassing any sort of random initialization, and ultimately poisons the resultant model.

The data hub scenario is similar, except the attacker no longer needs to get a prepoisoned model in the hands of the trainer; they let the trainer poison it themselves. This is likely the most analyzed attack scenario and has been shown feasible “in-the-wild”. One example of a real-world attack comes from modifying the IDMB review dataset to include hateful speech [24].

Many static datasets arise via snapshotting a large corpus of data. As previously mentioned, the Wikicommons dataset consists of data, snapshotted from Wikipedia, and packaged by Wikipedia to make downloads easier [25]. Recently

a feasible exploit was found that uses the period window for Wikipedia’s snapshotting operation, and injects poisonous mutations to the site just before the snapshot occurs and before the community would have time to review and correct. This attack then allows changes to the dataset such as the inclusion of hateful speech, misinformation, etc., to make it to the training set [26]. Similar attacks exist for images and artwork. In fact, poison attacks have even been proposed as a means to create evidence that a generative image tool has violated copyright infringement [27].

Finally, there have been attacks on loss functions. An attacker can inject code into a loss function that forces a bias in a way that favors an attacker’s goals [28]. This presents an attack that is very different in nature and whose mitigation needs to take a different course of action than the rest of the attacks mentioned here. This attack will thus not be mitigated by the current work.

In the remainder of this section, we discuss mitigations against poison attacks. One of the hardest aspects of mitigating poison attacks is akin to the reason that heap-spraying attacks are hard to detect. Heap-spray attacks are probabilistic in terms of how much of the heap to spray and whether one can find a latent defect that activates the sprayed-heap [29]. Likewise, in a dataset poison attack, an attacker manipulates only a fraction of the images, often as few as 0.1%, and there is no guarantee that the attack will always be successful [30]. We emphasize that one important aspect of engineering machine learning models in a safe way uses security standard practices, especially with regards to data. For example the PLOT4ai approach to threat modeling provides strategies for applying standard security best practices and data management to machine learning development [31]. There are even startups geared towards directly helping track data provenance and the entire data supply chain [32].

There are a couple areas where such standard, best-practices for security do not fully, adequately cover poison attacks. First, for example, in PLOT4ai, and related methodologies [31], the closest strategy for safe deployment relevant to dataset poisoning is tracking concept drift [33]. However, concept drift does not directly address poison attacks, since many poison attacks will not alter the model’s performance in validation. Further, with the number of opportunities presented by machine learning growing rapidly, and in an area where first to market takes precedence over getting to market safely, we need easy-to-apply mitigations that do not require developer input. Further, the standard procedures will not cover insider attacks nor spoofing attacks where a developer spoofs credentials or trustworthy names in the dataset repositories and modifies existing datasets. In other words, we need specialized mitigations that directly mitigate harm from dataset poisoning. Since the design of poison attacks often makes them hard-to-detect, an approach to mitigation that provides a guarantee on detection rates might be preferable to a mitigation strategy that seems to work, possibly even better, but has no guarantee. A guaranteed mitigation strategy could at least quantify the risk posed by poison since we could state exactly what kinds of attacks we prevent and provide a lower bound on the rate at which we detect. A guarantee for proactive dataset defense would ensure that starting from a clean dataset, one can expect it to prevent enough poison

from entering the stream so that the attack cannot become successful.

Given attack specific details, one can craft a defense mechanism, as in [34]–[36]. These specially crafted mitigations should not be downplayed; they provide important tools that can be used to mitigate specific attacks. Many attack specific mitigations use optimization-based techniques to identify and mitigate poisons that are themselves generated with an optimization-based technique; thus, they do not generalize well. One approach to reducing the effectiveness of training that does generalize well comes from differentially private learning; the idea being that by discounting the importance of subsequent examples seen during training, the poisoned examples’ effects also diminish [37]. One significant drawback of differentially private learning is that, currently, differentially private learning produces less performant models [38]. In some cases, such as when the differential privacy bounds are incompatible with the VC-dimension, one may be even able to prove that reduced performance is unavoidable; though, we are not aware of anyone having done this. Recent work has proposed a different, yet still generic approach for mitigating poison attacks, by noticing that often poisoned data creates significantly larger features in a model [4], [39]. These approaches then assume that training on poisoned data creates models where attacked inputs have the largest features. Based on this assumption, the problem of detecting and hence mitigating poisoned data can be formulated as an optimization problem with a guarantee of detecting poison. The downside, as mentioned earlier, is that detecting poison, using this technique, with a guarantee, requires solving an NP-complete problem in general and in practice the average running time was found to be entirely prohibitive [4]. To the best of our knowledge, there does not currently exist a mitigation scheme that has any guaranteed bound on detection rate that also has a known polynomial runtime. Thus, currently, the risk of data poisoning attacks to training machine learning systems cannot be genuinely quantified, and hence an organization cannot make an informed decision about whether the data they are using has become compromised [40].

3 Trigger poison attacks on labeled data

In this section, we define trigger-based poison attacks, henceforth called *trigger attacks* and review common notions from the literature.

Dataset poisoning is an attack on machine learning systems in which an attacker obtains access to a dataset and manipulates it through some means (thereby “poisoning” it), with the intent that a model trained on the poisoned dataset will mispredict in a way that the attacker can then exploit.

Often, researchers define dataset poisoning as an optimization problem [4], [5]. This may be helpful in understanding one way to perform attacks. Viewing poison *qua* optimization leaves unaddressed attacks that do not optimize an objective function (e.g. those that simply apply a batch to both inputs and labels, probabilistically). Second, it necessarily reduces any guaranteed detection to the task of finding absolutely optimal items; furthermore, finding the

most optimal items is typically equivalent to an NP-complete problem [4]. This leads to either using an approximation algorithm to the NP-complete problem or using heuristic, *ad hoc* detection methods neither of which have acceptable, guarantee-able detection rates. If instead, we slightly weaken this position, we find we can provide all the necessary definitions purely in terms of stochastic processes, and we will take this approach here.

3.1 Probabilistic Setting

A common assumption about datasets is that they arise from an IID sampling process on some underlying “data distribution”. However, in studying poisoning, we will need to weaken this position to allow an adversary to choose samples to manipulate and to then make those changes. Intuitively, we will not be able to formulate such an adversary’s actions from an IID point of view. We thus assume that we sample datasets *in toto*. I.e., we actually sample from a distribution on sequences of data, or equivalently that we have a random variable that is sequence valued. Individual elements of such sequences do have associated marginal distributions, but we do not make the assumption that they are independent. We allow for samples that have repeated elements and are therefore properly dealing with “multisets” instead of sets. We will now formalize this.

Let $\mathcal{X} = (\underline{\mathcal{X}}, \Sigma_{\mathcal{X}}), \mathcal{Y} = (\underline{\mathcal{Y}}, \Sigma_{\mathcal{Y}})$ be measurable spaces. For a measurable function $f: \mathcal{X} \rightarrow \mathcal{Y}$, we denote by $f^*: \Sigma_{\mathcal{Y}} \rightarrow \Sigma_{\mathcal{X}}$ the map that sends a measurable set U to its inverse image along f . The product space $\mathcal{X} \times \mathcal{Y}$ is the measurable space underlied by the set $\underline{\mathcal{X}} \times \underline{\mathcal{Y}}$ and which has the initial (smallest) σ -algebra such that the projections are measurable. We write $\mathcal{X}^n := (\underline{\mathcal{X}}^n, \Sigma_{\mathcal{X}^n})$ to denote the iterated power. Suppose $X: \Omega \rightarrow \mathcal{X}^n$ is any random variable, then by the product law, it splits as $X = \langle X_1, \dots, X_n \rangle$; hence, as a sequence of random variables of the form $X_j: \Omega \rightarrow \mathcal{X}$. From our intuition above, we want to be able to view the sequence $\langle X_1, \dots, X_n \rangle$ as a multiset. There are several ways to formalize this. For this paper, the notion of exchangeable random variable, which imposes invariance with respect to actions of the symmetric group S_n of permutations of $\{1, \dots, n\}$ on \mathcal{X}^n , suffices.

Definition 3.1. A probability distribution μ on \mathcal{X}^n is **exchangeable** when for every $\sigma \in S_n$ the following commutes.

$$\begin{array}{ccc} \Sigma_{\mathcal{X}^n} & \xrightarrow{\mu} & [0, 1] \\ \sigma^* \downarrow & & \uparrow \mu \\ \Sigma_{\mathcal{X}^n} & \xrightarrow{\mu} & [0, 1] \end{array}$$

That is, $\mu(\sigma^*(U)) = \mu(\{(x_{\sigma(1)}, \dots, x_{\sigma(n)}) \mid (x_1, \dots, x_n) \in U\}) = \mu(U)$.

Similarly, a sequence of random variables $X = \langle X_1, \dots, X_n \rangle$ as above is **exchangeable** when the pushforward measure $X_*\mu$ is an exchangeable distribution on \mathcal{X}^n .

Indeed a sequence of random variables $\langle X_1, \dots, X_n \rangle$ is exchangeable exactly when for every permutation σ , $\langle X_1, \dots, X_n \rangle$ and $\langle X_{\sigma(1)}, \dots, X_{\sigma(n)} \rangle$ are identically distributed. Thus, such a random variable is precisely a finite multiset of random variables to within distribution. A deeper relationship between multisets and exchangeable distributions is possible but not needed for this paper.

Observation 3.2. *Often in literature on conformal prediction, one will use the phrase, “assume z_1, \dots, z_{n+1} are generated from an exchangeable probability distribution on \mathcal{Z}^{n+1} .” From the above, we simply mean that z_1, \dots, z_{n+1} are a realization of some random variable $\langle Z_1, \dots, Z_{n+1} \rangle$ whose distribution is an exchangeable distribution on \mathcal{Z}^{n+1} ; or more simply, that we have an exchangeable random variable $\langle Z_1, \dots, Z_{n+1} \rangle$.*

In describing the mathematics behind dataset poisoning of, say, an image dataset, a naïve approach might model the attack as a function that applies a patch to some subset of images. However, many real-world attacks often do not work this way. For example, attacks often apply a stochastic optimization technique to choose the best images and pixels in those images to modify to accomplish their goal. To accurately describe such attacks, we need a way to capture something like a function but where there are stochastic elements applied as well. Markov kernels are a mathematical tool that provide exactly this. In fact, they are functions not from points to points, but from points to distributions.

Definition 3.3. *For measurable spaces, \mathcal{X}, \mathcal{Y} , a **Markov kernel** h , denoted $h : \mathcal{X} \dashrightarrow \mathcal{Y}$, is a measurable function $h : \mathcal{X} \rightarrow G(\mathcal{Y})$ where $G(\mathcal{Y})$ is the measurable space of all probability distributions on \mathcal{Y} .*

We give some examples now. First, every probability distribution gives rise to a Markov kernel.

Example 3.4 (Probability distributions). *Since a Markov kernel $\mathcal{X} \dashrightarrow \mathcal{Y}$ assigns to each point in \mathcal{X} a probability distribution on \mathcal{Y} , when \mathcal{X} is a one element set, a Markov kernel $\{*\} \dashrightarrow \mathcal{Y}$ is just a probability distribution on \mathcal{Y} .*

Another common example comes from deterministic functions; that is, if the relationship is an ordinary (measurable) function, then it is a Markov kernel.

Example 3.5 (Deterministic functions). *Every measurable function $f : \mathcal{X} \rightarrow \mathcal{Y}$ provides a kernel $k_f : \mathcal{X} \dashrightarrow \mathcal{Y}$ where $k_f(x)$ is the distribution on \mathcal{Y} which for an event $U \in \Sigma_{\mathcal{Y}}$ is defined as*

$$k_f(x)(U) := \begin{cases} 1 & f(x) \in U \\ 0 & \text{otherwise} \end{cases}$$

Another common example comes from discrete-time Markov chains (Markov chains over discrete sets). The transition function of a discrete-time Markov chain is described by a finite-dimensional stochastic matrix.

Example 3.6 (Stochastic matrices). Let \mathcal{X}, \mathcal{Y} be discrete spaces with $|\mathcal{X}| = m$ and $|\mathcal{Y}| = n$. A Markov kernel $\mathcal{X} \rightarrow \mathcal{Y}$ is then, for each $x \in \mathcal{X}$, a discrete probability distribution, h_x on \mathcal{Y} . Then each h_x provides a list of length n that sums to 1, so that we obtain an n -row, m -column matrix h where each column sums to 1, which is precisely a stochastic matrix/the transition function for a discrete-time Markov chain.

Another example, that will be used throughout this paper, describes the possibility that an adversary might probabilistically split a dataset into items that will be poisoned and those that will not be poisoned.

Definition 3.7. A *splitting* of a measurable space \mathcal{Z} consists of integers $0 < k < n$ together with Markov kernels $\dagger: \mathcal{Z}^n \dashrightarrow \mathcal{Z}^n$ and $\uplus: \mathcal{Z}^n \dashrightarrow \mathcal{Z}^n$ such that

$$\begin{array}{ccc} \mathcal{Z}^n & \xrightarrow{\dagger} & \mathcal{Z}^n \\ & \searrow & \downarrow \phi_{\uplus} \\ & & \mathcal{Z}^n \end{array}$$

where the composition is qua Markov kernels.

3.2 What is a trigger attack?

Let \mathcal{X} and \mathcal{Y} be measurable spaces. A **labeled dataset** D of width n is an exchangeable random variable $\langle (X_1, Y_1), \dots, (X_n, Y_n) \rangle: \Omega \rightarrow (\mathcal{X} \times \mathcal{Y})^n$. The intent is that a realization of such a variable is a multiset of pairs of the form (x, y) where x is viewed as an example input and y is the desired label. In the current work, we will restrict to the case where \mathcal{Y} is finite; in practice this means we restrict to classification datasets and do not work with regression nor time-series datasets.

We will often assume datasets D are split as a disjoint union $D := D_P \uplus D_C$ — we will think of D_P as the items that are going to be poisoned (eventually) and D_C as the clean items that will not be poisoned. However, a clever attacker will often artfully choose which items to attack, and this choice of which items to manipulate can become an integral part of the attack [2], [3]. We thus assume that the splitting of D is provided by a *splitting* in the sense of Definition 3.7.

We review common examples of splittings. We start first with a deterministic splitting.

Example 3.8. A simple attack scenario on a facial recognition system provides a completely deterministic (non-random) splitting. Suppose a company trains its facial recognition system to recognize only employees' faces using a dataset of n face image samples. An attacker wants to sneak an existing employee, named X -Doe, into an area where they do not have access, but Mgr does. They may use a splitting scheme where they just select the first k X -Doe pictures to make D_P and the remaining $n - k$ comprise D_C .

A modification of the above scenario gives rise to an attack where randomness plays a role in the splitting. In this scenario, we want to ensure that the

attack applies not only to a single entity, but can be applied generally to any entity.

Example 3.9. *The company is still training their facial recognition software to recognize only employees' faces. This time, they want to get a non-employee into the building by getting them recognized as a legitimate employee. The attacker may randomly choose up to k images to make D_P and the remaining $n - k$ images comprise D_C .*

The Witches' Brew attack [3] provides a more sophisticated use of randomness in the splitting. In this scenario, the attacker will optimize over which images to attack so that their attack can potentially succeed with fewer images changed and with fewer changes to those images.

Example 3.10. *Given a dataset of images, seed a random-number generator, apply a stochastic optimization technique to select the k best images to modify by the smallest changes possible while triggering the desired misclassification.*

We will often denote by M_D the result of training some model architecture M on a dataset D .

Definition 3.11. *A **trigger poison attack** on labeled data $\mathcal{X} \times \mathcal{Y}$ consists of a splitting \dagger of $\mathcal{X} \times \mathcal{Y}$ together with a pair of Markov kernels of type*

$$\mathcal{X} \xleftarrow[t_0]{\circ} \mathcal{X} \times \mathcal{Y} \xrightarrow[t_1]{\circ} \mathcal{Y}$$

We write t for the induced map

$$t := \mathcal{X} \times \mathcal{Y} \xrightarrow[\circ]{\langle t_0, t_1 \rangle} \mathcal{X} \times \mathcal{Y}$$

(called a **trigger**). Let $\mathcal{Z} := \mathcal{X} \times \mathcal{Y}$. The poison attack gives rise to a composite of Markov kernels

$$\mathcal{Z}^n \xrightarrow[\circ]{\dagger} \mathcal{Z}^k \times \mathcal{Z}^{n-k} \xrightarrow[\circ]{t^k \times \text{id}} \mathcal{Z}^k \times \mathcal{Z}^{n-k} \xrightarrow[\circ]{\text{w}} \mathcal{Z}^n$$

In Definition 3.11, note that Markov kernels only have weak products; $\langle t_0, t_1 \rangle$ is merely shorthand for

$$\mathcal{X} \times \mathcal{Y} \xrightarrow[\circ]{\Delta} (\mathcal{X} \times \mathcal{Y}) \times (\mathcal{X} \times \mathcal{Y}) \xrightarrow[\circ]{t_0 \times t_1} \mathcal{X} \times \mathcal{Y}$$

and where in general $\Delta : \mathcal{W} \xrightarrow[\circ]{\circ} \mathcal{W} \times \mathcal{W}$ is the kernel which for each $w \in \mathcal{W}$ provides a probability distribution $\Delta(w)$ such that

$$\Delta(w)(U \times V) := \begin{cases} 1 & w \in U \cap V \\ 0 & \text{otherwise} \end{cases}$$

Here are some common examples of triggers. The first continues Example 3.8 so that X-Doe can apply face-paint that looks like the patch whenever they want to gain access to the Mgr section.

Example 3.12. For each image in D_P , place a small rectangular patch on the face of X -Doe at the exact same coordinates in every image.

A randomized trigger can be found by continuing Example 3.9. Here we allow variance in the attack so that the model doesn't learn to only look in a specific spot, but learns to recognize the patch across different face and different locations.

Example 3.13. We apply the same sort of rectangular patch to the k selected images as in Example 3.12; however, instead of applying the attack at the same coordinates, we randomly choose the coordinates to attack.

A more subtle example can be found by continuing Example 3.10.

Example 3.14. In the Witches' Brew attack [3], the stochastic optimization procedure determines the splitting out of the k images and also what pixels to attack and by how much. Thus, the trigger here is also stochastic.

One might object that this is not the most general form of a poison attack; for instance, it does not cover attacks that add items to the dataset to force undesired, spurious correlations [2]. A subtler attack not directly captured by the above is one where the success separates the attacked label and the desired label: where the t_y is not the label the attacker seeks to induce (these would be incorrectly counted as ineffective in the current framework). Note that while such attacks make sense within our framework, and can even be detected, they do not come with a straightforward notion of success rate. One would need to develop a more nuanced notion of success rate by tying it to a specific feature (i.e., making it conditional), which we leave for future work. Still the trigger attack is one of the more convincing due to the feasibility of real-world execution with less chance of raising suspicions (e.g., if the Wikipedia dataset suddenly got larger, then that would be alarming).

3.3 Conformal Separability

We will now introduce a general tool for hypothesis testing on datasets that we call *Conformal Separability* and will derive our *Conformal Separability Test* (Algorithm 1). We will use the Conformal Separability Test to prove Theorem 3.39 which states that an effective attack is always detectable with a finite sample validity guarantee.

This tool builds on conformal prediction [41], [42]. At a high-level, conformal prediction provides a framework for rigorously, statistically analyzing machine learning algorithms with probabilistic guarantees. Researchers have noticed a strong link between conformal prediction and anomaly detection [43]. Conformal prediction allows detecting deviations from *exchangeability*. Exchangeability forces identically distributed marginals; hence, has been used to detect distribution-shift in distribution-free settings. Many of the applications of conformal prediction to anomaly detection consider the case where the sets of predictions are singletons (so called confident predictions). However, when applying

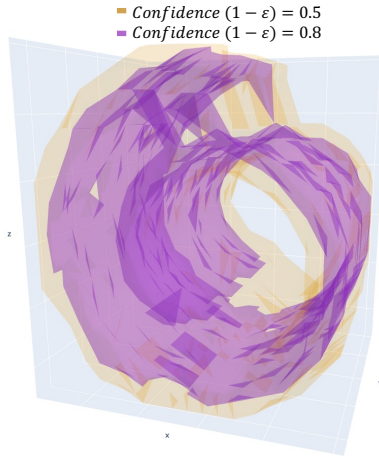


Figure 3: An approximate visualization of conformal prediction sets at two confidence levels for the Swiss-roll dataset.

conformal prediction to neural networks, one often obtains sets with more than one element. For example, [44] suggests that on some datasets, nearly 40% of items have non-singleton prediction sets. We designed the Conformal Separability Test to circumvent this multiple label problem; that is, to enable poison detection even when the prediction is not “confident”, thus making this more general than anomaly detection.

We refer the reader to [41], [45] for details on conformal inference in general. We sketch the central idea behind conformal prediction in Figure 3.

Conformal prediction sets provide a set estimator in the distribution-free context that only requires two mild assumptions: that there is a measurable test of *non-conformity* (a so-called *non-conformity score*) and that our training datasets are exchangeable.

Definition 3.15. *A non-conformity score is a family of measurable functions*

$$A := \{(\mathcal{X} \times \mathcal{Y})^n \times \mathcal{X} \times \mathcal{Y} \xrightarrow{A_n} \mathcal{R} \mid n \in \mathbb{N}\}$$

such that for each A_n and for all $\sigma \in S_n$,

$$A((b_1, \dots, b_n), x, y) = A((b_{\sigma(1)}, \dots, b_{\sigma(n)}), x, y)$$

We provide a few examples of non-conformity scores.

Example 3.16. *Suppose that \mathcal{Y} is finite and that there is a \mathcal{Y} dependent distance on \mathcal{X} ; i.e. there is a metric $d_y(_, _)$ for each $y \in \mathcal{Y}$. Then for each (b_1, \dots, b_n) , we obtain a non-conformity score by taking*

$$A_n((b_1, \dots, b_n), x, y) = d_y(x, \text{centroid}_y(b_1, \dots, b_n))$$

where $\text{centroid}_y(b_1, \dots, b_n)$ is the centroid of the set of points (x_j, y) for $b_j = (x_j, y_j)$ with respect to the metric d_y .

The following example of a non-conformity score is often viewed as incredibly impractical.

Example 3.17. Suppose D is an exchangeable random variable in $\mathcal{R}^{\text{in-dim}} \times \mathcal{R}^{\text{lab-dim}}$. Write M_D for the result of training a neural network on D with full backpropagation on mean square error and a fixed learning rate l and fixed weight initialization. Then we obtain a non-conformity score:

$$A(D, x, y) = d(M_D(x), y)$$

where d is the euclidean distance on $\mathcal{R}^{\text{out-dim}}$. This is symmetric in d since we apply full backpropagation over the entire dataset at once.

Note that we can swap mean square error in the above with any symmetric loss function.

If one were to apply stochastic gradient descent or split D into multiple batches, one would need a convergence result to provide any sense in which A is symmetric in the first n arguments. Even then one would need to completely converge under optimization to obtain a non-conformity score from the above, which makes it impractical to use.

To get around these issues and to simultaneously overcome the need to fully retrain a neural network on each application, one often moves to a so-called inductive score, which we present as the following family of examples. See for example, [41], [44], [45] for concrete uses of inductive conformal prediction on neural networks.

Example 3.18. Suppose $A := \{A_n : (\mathcal{X} \times \mathcal{Y})^n \times \mathcal{X} \times \mathcal{Y} \rightarrow \mathcal{R} \mid n \in \mathbb{N}\}$ is a family of measurable functions (note we are not assuming A_n is symmetric in its first n arguments). Then for any $D_0 \in (\mathcal{X} \times \mathcal{Y})^m$, we get a proper non-conformity score $A_n^{D_0} : (\mathcal{X} \times \mathcal{Y})^n \times \mathcal{X} \times \mathcal{Y} \rightarrow \mathcal{R}$ by sending $D \in (\mathcal{X} \times \mathcal{Y})^n$ to

$$A_n^{D_0}(D, x, y) := A_n(D_0, x, y)$$

Note $A_n^{D_0}$ is trivially symmetric in D since it discards it entirely.

The above is certainly non-trivial since using it has the same validity theorem as for starting with an ordinary non-conformity score; however, one should keep in mind that they are essentially preconditioning the score on D_0 when stating conclusions.

A vital ingredient in performing conformal prediction is the p-value function.

Definition 3.19. Let A be a non-conformity score. For each n we obtain a measurable function $p_{n,A} : (\mathcal{X} \times \mathcal{Y})^n \times \mathcal{X} \times \mathcal{Y} \rightarrow [0, 1]$, called the *p-value function*, defined by setting $b := (b_1, \dots, b_n, (x, y))$ and then

$$p_{n,A}((b_1, \dots, b_n), x, y) := \frac{|\{i \mid A_{n+1}(b, (x_i, y_i)) \geq A_{n+1}(b, (x, y))\}|}{n + 1}$$

We call attention to the fact that $p_{n,A}$ is a $[0, 1]$ -valued random variable; whence, the preimage of any generator is measurable. In particular, *conformal prediction sets* are defined using preimages of the p -value function.

Definition 3.20. *Given a non-conformity score A , the **conformal prediction set** $\Gamma_{n,A}^\epsilon$ is defined as follows:*

$$\Gamma_{n,A}^\epsilon := p_{n,A}^*((\epsilon, 1])$$

Observation 3.21. *In the literature on conformal prediction, conformal prediction sets are often described in uncurried form. In this form, we have a sample D from the exchangeable distribution in question, and we write*

$$\Gamma_{n,A}^\epsilon(D) := \{(x, y) \mid p_{n,A}(D, x, y) > \epsilon\}$$

When D is a random variable then

$$\Gamma_{n,A}^\epsilon \equiv \{(z_1, \dots, z_{n+1}) \mid z_{n+1} \in \Gamma_{n,A}^\epsilon(z_1, \dots, z_n)\}.$$

We can also use DeFinetti notation for events and write $\{p_{n,A} > \epsilon\}$, $\{Z_{n+1} \in \Gamma\}$. In this way, for random variables, Z_1, \dots, Z_{n+1} , we can equate the events

$$\{p_{n,A} > \epsilon\} \equiv \{Z_{n+1} \in \Gamma_{n,A}(Z_1, \dots, Z_n)\} \equiv \Gamma_{n,A}^\epsilon$$

In fact a further uncurrying is even used.

$$\Gamma_{n,A}^\epsilon(D, x) := \{y \mid p_{n,A}(D, x, y) > \epsilon\}$$

The final version requires more care when making probabilistic statements. In particular we have no a priori assumptions on the (marginal) distributions on the product space $\mathcal{X} \times \mathcal{Y}$ other than that \mathcal{Y} is finite as used in, e.g., [41], [46] for establishing validity when we uncurry all the way to the last x .

Below, given a random variable $\langle Z_1, \dots, Z_{n+1} \rangle : \Omega \rightarrow (\mathcal{X} \times \mathcal{Y})^{n+1}$, we denote by $\mathbb{P}_{\langle Z_1, \dots, Z_{n+1} \rangle}$ the pushforward measure on $(\mathcal{X} \times \mathcal{Y})^{n+1}$.

Theorem 3.22. [Vovk et al. [41], [42], [47]] *For any exchangeable sequence of variables $\langle Z_1, \dots, Z_{n+1} \rangle : \Omega \rightarrow (\mathcal{X} \times \mathcal{Y})^{n+1}$, we have*

$$\mathbb{P}_{\langle Z_1, \dots, Z_{n+1} \rangle}(\Gamma_{n,A}^\epsilon) \geq 1 - \epsilon$$

Proof. See [42], [48] for a proof. □

Using the more common notation in the literature, described in Observation 3.21, we would write $\mathbb{P}_{\langle Z_1, \dots, Z_{n+1} \rangle}(Z_{n+1} \in \Gamma_{n,A}^\epsilon(Z_1, \dots, Z_n)) \geq 1 - \epsilon$ instead of the form given in Theorem 3.22.

The above uses the (exchangeable) distribution induced by the exchangeable random variable $\langle Z_1, \dots, Z_{n+1} \rangle$, but we could equally well pull this straight back to the latent probability space Ω :

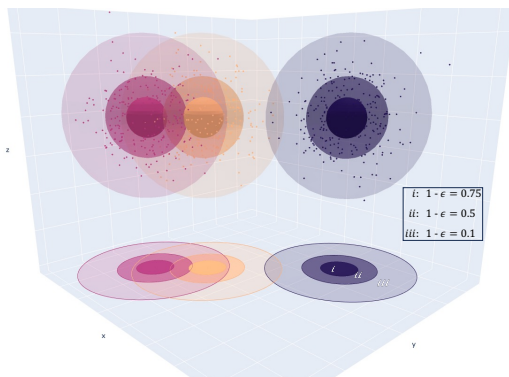


Figure 4: Visualization of Conformal Separability. Conformal Separability is a conservative test for inequality of conformal prediction sets. Here the magenta and orange sets are not conformally separable until confidence is high. The blue and orange spheres are much more separable, as they do not overlap until the confidence becomes remarkably low. For the red and blue to overlap; one would need astronomically low confidence. This is akin to the test for normal distribution separation checking overlap of confidence intervals; but we are porting this to a distribution-free setting where the test is over arbitrarily irregular distributions on manifolds of high-dimension.

Corollary 3.23. *Given $\langle Z_1, \dots, Z_{n+1} \rangle : \Omega \rightarrow (\mathcal{X} \times \mathcal{Y})^{n+1}$, an exchangeable sequence of random variables, $\mathbb{P}_\Omega(\langle Z_1, \dots, Z_{n+1} \rangle^* (\Gamma_{n,A}^\epsilon)) \geq 1 - \epsilon$.*

We depict the intuitive idea behind the Conformal Separability Test in Figure 4. There are less conservative tests than this, but they require making additional trade-offs (e.g., fixing a model or accepting additional computation). For example, 2-sample t -tests (e.g., the Welch’s test) can detect significant difference with small p-values for largely overlapping confidence intervals, and one can do even better when the variances are known to be the same or close.

In the following, we let \mathbb{P}_{D_1, D_2} , where $|D_1| = n$ and $|D_2| = m$, denote the induced (pushforward) measure

$$\Sigma_{\mathcal{Z}^n \times \mathcal{Z}^m} \xrightarrow{\langle D_1, D_2 \rangle^*} \Sigma_\Omega \xrightarrow{\mathbb{P}} [0, 1].$$

Let $\Delta : \Omega \rightarrow \Omega \times \Omega$ be $\omega \mapsto (\omega, \omega)$. Then $\Delta^*(U \times V) = U \cap V$. Then factor $\langle D_1, D_2 \rangle : \Omega \rightarrow \mathcal{Z}^n \times \mathcal{Z}^m$ as

$$\langle D_1, D_2 \rangle = \Omega \xrightarrow{\Delta} \Omega \times \Omega \xrightarrow{D_1 \times D_2} \mathcal{Z}^n \times \mathcal{Z}^m.$$

Thus $\mathbb{P}_{D_1, D_2}(U \times V) = \mathbb{P}(D_1^*(U) \cap D_2^*(V))$ for every $U \in \Sigma_{\mathcal{Z}^n}, V \in \Sigma_{\mathcal{Z}^m}$. Thus \mathbb{P}_{D_1, D_2} is canonically measuring an intersection event. We may sometimes write simply $\mathbb{P}_{D_1, D_2}(U, V)$.

Definition 3.24. Let a non-conformity score A be given and assume D_1 and D_2 are sequences of random variables. Fix $\epsilon, \gamma, \delta \in (0, 1)$. D_1 and D_2 are **A -conformal $(\epsilon, \gamma, \delta)$ -separable** when

$$\mathbb{P}_{D_1, D_2}(\Gamma_{n_1, A}^\epsilon, \Gamma_{n_2, A}^\gamma) < \delta,$$

where \mathbb{P}_{D_1, D_2} is the probability distribution induced by D_1 and D_2 .

Since $\epsilon, \gamma, \delta > 0$, when D_1 and D_2 have an $(\epsilon, \gamma, \delta)$ -separator, they are unequal on a non-measure zero set, hence they are not almost surely equal.

Crucially, exchangeability forces an upper bound on separability.

Theorem 3.25. Let A be a non-conformity score and suppose $D_1 : \Omega \rightarrow \mathcal{Z}^n$ and $D_2 : \Omega \rightarrow \mathcal{Z}^m$ are independent as two sequence-valued random variables such that each of D_1 and D_2 are individually exchangeable. Then D_1 and D_2 cannot be A -conformal $(\epsilon, \gamma, \delta)$ -separable for any $\delta < (1 - \epsilon)(1 - \gamma)$.

Note that Theorem 3.25 does *not* assume that D_1 and D_2 are individually IID; we are only assuming that, individually, they are exchangeable, and that as random variables valued in sequences these sequences are independent.

Proof. The proof follows nearly immediately from independence and Theorem 3.22:

$$\mathbb{P}_{D_1, D_2}(\Gamma_{n, A}^\epsilon, \Gamma_{m, A}^\gamma) = \mathbb{P}_{D_1}(\Gamma_{n, A}^\epsilon) \cdot \mathbb{P}_{D_2}(\Gamma_{m, A}^\gamma) \geq (1 - \epsilon) \cdot (1 - \gamma).$$

□

In Theorem 3.25, we are measuring a set of the form $A \cap B$. Also recall that for conformal prediction we view measuring $\Gamma_{n, A}^\epsilon$ intuitively as $Z_{n+1} \in \Gamma_{n, A}^\epsilon$. Strictly speaking, that statement is not well typed since as a set $Z_{n+1} \in \Gamma_{n, A}^\epsilon$ iff $p(D, Z_{n+1}) > \epsilon$, hence the event defined by the indicator of those predicates coincides. To have a similar intuition for separability, and indeed, to define the test, we need to ensure that the last random variable of each sequences is the same. The following is as such a consequence of Theorem 3.25. Thus if we have random variables of the form $\langle D_1, Z_\nu \rangle$ and $\langle D_2, Z_\nu \rangle$, we may soundly write $Z_\nu \in \Gamma_{n+1, A}^\epsilon(D_1) \cap \Gamma_{m+1, A}^\gamma(D_2)$ for the pullback of $[0, \epsilon) \times [0, \gamma)$.

Corollary 3.26. Let A be a non-conformity score and suppose $\langle D_1, Z_\nu \rangle : \Omega \rightarrow \mathcal{Z}^{n+1}$ and $\langle D_2, Z_\nu \rangle : \Omega \rightarrow \mathcal{Z}^{m+1}$ are independent as two sequence valued random variables such that both D_1, D_2 are individually exchangeable. Then $\langle D_1, Z_\nu \rangle$ and $\langle D_2, Z_\nu \rangle$ cannot be A -conformal $(\epsilon, \gamma, \delta)$ -separable for any $\delta < (1 - \epsilon) \cdot (1 - \gamma)$. Equivalently,

$$\mathbb{P}_{\langle D_1, Z_\nu \rangle, \langle D_2, Z_\nu \rangle}(Z_\nu \in \Gamma_{n, A}^\epsilon(D_1) \cap \Gamma_{n, A}^\epsilon(D_2)) \geq (1 - \epsilon) \cdot (1 - \gamma)$$

Theorem 3.25 and Corollary 3.26 immediately determine an algorithm, our *Conformal Separability Test*, for testing separability. Observe the probability measurement of Γ , for a sequence valued random variable D , can be reformulated

Algorithm 1 Conformal Separability Test

Input: Data samples $D_i = (x_1, y_1), \dots, (x_{n_i}, y_{n_i})$, for $i = 1, 2$ to be compared

Input: Non-conformity score A

Input: Test input x

Output: $p_{\cap}(D_1, D_2, x)$

$p_{\cap}(D_1, D_2, x) := 0$

for $y \in Y$ **do**

for $i \in [1, 2]$ **do**

$p_{i,y} := p_A^{D_i}(x, y)$

end for

$p_{\cap}(D_1, D_2, x) := \max(p_{\cap}(D_1, D_2, x), \min(p_{1,y}, p_{2,y}))$

end for

return $p_{\cap}(D_1, D_2, x)$

as $\mathbb{P}_D(p_{n,A} > \epsilon) \geq 1 - \epsilon$. Note that p is a real-valued random variable and hence, by completeness of the reals, we can take its cádlág completion $\overline{p_{n,A}}$ and observe that $\mathbb{P}_D(\overline{p_{n,A}} \geq \epsilon) \geq 1 - \epsilon$. For a brief introduction to the cádlág completion see Exercises 5.13, 5.14 in Chapter 1 and 1.17–1.21 in Chapter 2 of [49].

However, this can then be immediately reformulated in terms of the CDF of $\overline{p_{n,A}}$, denoted by $F_{p_{n,A}}$:

$$1 - F_{p_{n,A}}(\epsilon) = 1 - \mathbb{P}_D(p_{n,A} \leq \epsilon) = \mathbb{P}_D(\overline{p_{n,A}} \geq \epsilon) \geq 1 - \epsilon.$$

This implies that $F_{p_{n,A}}(\epsilon) \leq \epsilon$.

Observe that we have the following identity

$$\mathbb{P}_{D_1, D_2}(\Gamma_{n,A}^\epsilon, \Gamma_{m,A}^\epsilon) = 1 - F_{\min(p_{n,A}, p_{m,A})}(\epsilon).$$

This allows us to state the correctness for Algorithm 1 as follows.

Theorem 3.27. *Let $p_{\cap}(D_1, D_2, x)$ denote the output of Algorithm 1. Then $\|p_{\cap}(D_1, D_2, x) - \mathbb{P}(\Gamma_{n,A}^\epsilon, \Gamma_{m,A}^\epsilon)\|_{\infty} \rightarrow 0$ almost surely.*

Proof. This is a special case of the Glivenko-Cantelli theorem [50]–[52], applied to Algorithm 1, which computes $1 - E$ where E is the empirical CDF for $\min(p_{n_1,A}, p_{n_2,A})$. \square

A finite sample version of the above can be obtained from the the Dvoretzky-Kiefer-Wolfowitz inequality [53], applied to Algorithm 1, noting again that it computes the complement of the empirical CDF (i.e. the empirical version of $1 - F_{\min(p_{n_1,A}, p_{n_2,A})}$). The finitary bound incurs another constant and makes carrying it around harder. We can work with the asymptotic version in this paper, since it is an asymptotic result about convergence for a finite sample result.

3.4 Empirical detection of poison attacks using conformal separability

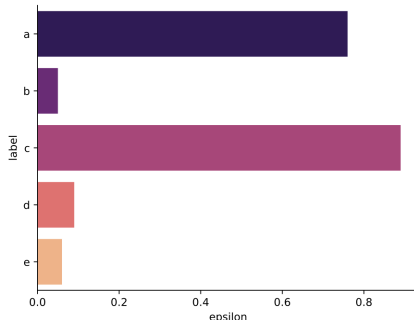
We will now consider notions of effective attack. We will show that when given a dataset random variable D and when P denotes a trigger attack applied to D , that D, P are conformally separable. In particular, we will show that the event of observing an empty intersection between conformal prediction sets is a rare event. Moreover, an effective attack forces this intersection to be empty. It then follows immediately that if on average the attack is successful, then in expectation we will always see a rare event!

Before proceeding, we fix notation. As before, we assume that $D : \Omega \rightarrow (\mathcal{X} \times \mathcal{Y})^{n+1}$ is an exchangeable random variable. As common in statistics literature, we will identify samples from the distribution induced by D with the random variable D . This is a convenient abuse of notation since then the sample distribution of D is precisely the distribution induced by D . Likewise, if we post-compose any D_i with the trigger t (in the sense of Def. 3.11), we induce a distribution on $\mathcal{X} \times \mathcal{Y}$. We will denote the realizations of such samples by (t_{x_i}, t_{y_i}) . We will denote by P , samples from the induced “poisoned” distribution on $(\mathcal{X} \times \mathcal{Y})^{n+1}$. In this section, we adopt the abbreviation $p^D(x, y)$ for the p-value $p_{n,A}(D, (x, y))$.

Definition 3.28. *Given a nonconformity score A , dataset D and $x \in \mathcal{X}$ we define the **expiry of x for D** to be the random map $\tau^D(x)$ sending y to $p^D(x, y)$. In our case, \mathcal{Y} is finite and we interpret $\tau^D(x)$ as a random vector in $\mathcal{R}^{|\mathcal{Y}|}$.*

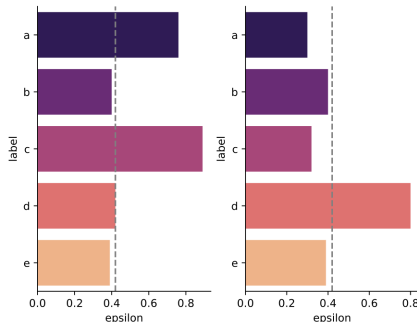
We can now give extra conditions that make detecting separation easy, and also relate this to the test for poison.

Example 3.29. *Suppose the set \mathcal{Y} consists of labels a, b, c, d , and e with and the corresponding p-values for some x are 0.76, 0.05, 0.89, 0.09, and 0.06. Then we visualize $\tau^D(x)$ as follows:*



This gives a picture of the conformal prediction set at x and identifies exactly when a label leaves the set.

Expiry determines the separability of sets. For example, suppose we are given D_1, D_2, x with expiry as indicated in the following figure:



The dashed line indicates the ϵ at which x is a separator; the colors to the right of the dotted line make it in the intersection at each ϵ .

We will now describe how Algorithm 1 can be used for the detection of poison attacks and we will then evaluate the mathematical implications of Theorem 3.27 to this application. To this end, we will first formalize the notion of what it means for an attack to be effective. As above, we assume that A is a fixed non-conformity score throughout this section and we caution that many of the notions defined below depend on the choice of A . We also maintain the notation that D is split as $D = D_C \uplus D_P$ and that $P := D_C \uplus t(D_P)$. In this section, any *attack* referenced will be of the form given in Definition 3.11.

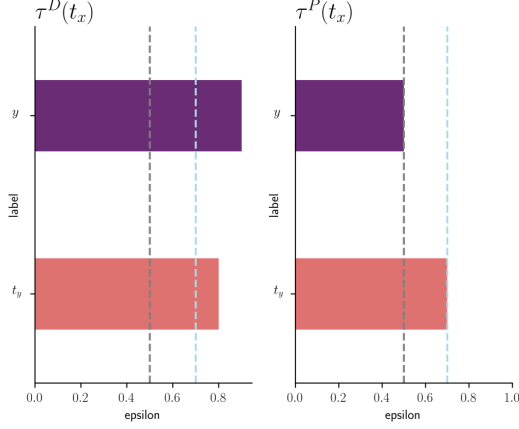
Definition 3.30. A trigger attack is **non-trivial** at (x, y) when $p^D(t_x, t_y) < p^D(t_x, y)$.

By the strictness of the inequality in Definition 3.30, we have that $y \neq t_y$ giving an immediately obvious sense of non-triviality. However, ultimately we want that t_y will end up being the strongest label when using the poisoned dataset P , and this notion of non-triviality also requires that t_y is not the strongest label to begin with. In other words, the attack will have to change a “belief” in order to be considered effective. This brings us to define notions of effectiveness.

Definition 3.31. A trigger attack is **weakly effective** at (x, y) , when $p^P(t_x, y) < p^P(t_x, t_y)$.

Note that *weakly effective* at (x, y) means that, in terms of expiry, the label t_y expires after y . However, it does not indicate that the attack was confidently successful. An attack is then intuitively effective when t_y is the most confident label in τ^P . However, one should wonder if this notion alone captures attack effectiveness.

Example 3.32. The following expiry provides a sort of counterexample to bounding the confidence one may have in attack effectiveness given non-triviality and weak effectiveness alone:



The first problem is that for the entire region for which $t_y \in \Gamma^P$ and $y \notin \Gamma^P$ (between grey and lightblue), we have $t_y \in \Gamma^D$, hence not separable within that region. Second, while the attack is formally effective, our confidence in t_y decreased after the attack. While this is not a problem for separation per se, it is a problem for bounding our confidence in separation.

The above example indicates that, in addition to requiring t_y to be the most confident label, we need to take into account both τ^D, τ^P simultaneously when creating a meaningful notion of effective. One possibility is to force relations like $p^P(t_x, t_y) > p^D(t_x, t_y)$. We instead capture the effectiveness in a more general form, and to do so we make it quantitative.

Definition 3.33. An attack is *empirically* $(1 - r)$ -effective at (x, y) given D, P when

$$[\text{re.1}] \quad p^D(t_x, t_y) < \min(r, p^D(t_x, y));$$

$$[\text{re.2}] \quad \max(\tau^P(t_x) - t_y) \leq r < p^P(t_x, t_y),$$

where we denote by $\tau^P(x) - y$ the vector obtained by projecting $\tau^P(x)$ onto the subspace corresponding to all but the y -th component.

Intuitively, an attack is empirically $(1 - r)$ -effective when Γ_ϵ^P is at most the singleton $\{t_y\}$ and $t_y \notin \Gamma_\epsilon^D$ for $\epsilon > r$.

Lemma 3.34. An empirically $(1 - r)$ -effective attack is both non-trivial and weakly effective.

Proof. Suppose an attack is empirically $(1 - r)$ -effective. Since

$$p^D(t_x, t_y) < \min(r, p^D(t_x, y)) \leq p^D(t_x, y),$$

the attack is non-trivial. Since $p^P(t_x, t_y) > r \geq \max(\tau^P(t_x) - t_y)$ we have that $p^P(t_x, t_y) > p^P(t_x, y)$ for any $y \neq t_y$. Since the attack is non-trivial, $t_y \neq y$, hence the attack is weakly effective. \square

The intuition behind a poisoned item being the most “dominant feature” can also be captured by requiring that $p^P(t_x, t_y) > \max(\tau^D(t_x))$. This kind of assumption, which mirrors assumptions in [4], forces empirical $(1-r)$ -effectiveness.

Lemma 3.35. *Suppose that an attack is non-trivial at (x, y) and additionally satisfies*

$$\max(\tau^P(t_x) - t_y) < p^P(t_x, t_y) \quad (1)$$

$$\max(\tau^D(t_x)) < p^P(t_x, t_y). \quad (2)$$

Then the attack is empirically $(1-r)$ -effective at (x, y) for some r .

Proof. Define

$$r := \max(p^D(t_x, y), \max(\tau^P(t_x) - t_y)).$$

To begin, [re.2] is an immediate consequence of (1) and (2). Then note that $\min(\max(a, b), a) = a$ for any a, b . Hence $\min(r, p^D(t_x, y)) = p^D(t_x, y)$. Then [re.1] follows from non-triviality. \square

In fact the r defined in the proof of Lemma 3.35 typically much larger than needed. Indeed, in practice $p^D(t_x, t_y)$ and $\max(\tau^D(t_x) - t_y)$ are both very small, and quite comparable. We can then push the r much lower depending on the relationship that these two quantities have.

Observation 3.36. *Suppose an attack is non-trivial at (x, y) . Then*

- (i) *If conditions (1),(2) of Lemma 3.35 hold, then the attack is always empirically $1-r$ effective for any r with $\max(p^D(t_x, t_y), \max(\tau^P(t_x) - t_y)) < r < p^P(t_x, t_y)$;*
- (ii) *If Lemma 3.35.(1) holds and additionally, $p^D(t_x, t_y) < \max(\tau^P(t_x) - t_y)$, then the attack is $1-r$ effective for $r := \max(\tau^P(t_x) - t_y)$;*
- (iii) *If Lemma 3.35.(2) holds and additionally, $\max(\tau^P(t_x) - t_y) < p^D(t_x, t_y)$ then the attack is empirically $1-r$ effective for any r with $p^D(t_x, t_y) < r < p^P(t_x, t_y)$.*

Proof. For (i). First note that from (1),(2) we have

$$\max(p^D(t_x, t_y), \max(\tau^P(t_x) - t_y)) \leq \max(\max(\tau^D(t_x)), \max(\tau^P(t_x) - t_y)) < p^P(t_x, t_y)$$

so that the interval $(\max(p^D(t_x, t_y), \max(\tau^P(t_x) - t_y)), p^P(t_x, t_y))$ is non-empty and therefore such an r exists. [re.1] then holds by non-triviality and construction of r and [re.2] holds by construction of r .

For (ii), [re.1] holds by construction and non-triviality and [re.2] follows immediately from (1).

For (iii), note that such r exist by (2). [re.1] then holds by construction and non-triviality. [re.2] holds: $\max(\tau^P(t_x) - t_y) < p^D(t_x, t_y) < r < p^P(t_x, t_y)$ by assumption followed by the construction of r . \square

Note that when an attack is $(1-r)$ -effective we have the following.

Lemma 3.37. *Suppose an attack is empirically $(1-r)$ -effective at (x, y) , given D, P . Then $\Gamma_n^r(D)(t_x) \cap \Gamma_n^r(P)(t_x) = \emptyset$.*

Proof. Suppose an attack is $(1-r)$ -effective at (x, y) . From [re.1], $t_y \notin \Gamma_n^r(D)(t_x)$. From [re.2], $\Gamma_n^r(P)(t_x) = \{t_y\}$, completing the proof. \square

From the above we know that an empirically effective attack forces the intersection of two prediction sets to be empty. However, we have not shown that we should be surprised by this. The following lemma shows that under an assumption of independence of samples, this is a rare situation.

Lemma 3.38. *Suppose that $\langle D_1, (X_{n+1}, Y_{n+1}) \rangle, \langle D_2, (X_{n+1}, Y_{n+1}) \rangle$, as $(\mathcal{X} \times \mathcal{Y})^{n+1}$ -valued random variables are independent in $(\mathcal{X} \times \mathcal{Y})^{n+1}$. Suppose also that both sequences are exchangeable. Then observing $p_{\cap}(D_1, D_2, x) \leq \epsilon$, (i.e. $\Gamma_n^\epsilon(D_1)(x) \cap \Gamma_n^\epsilon(D_2)(x) = \emptyset$) is $1 - (1 - \epsilon)^2$ -rare. The probability of $p_{\cap}(D_1, D_2, _) \leq \epsilon$ is less than $1 - (1 - \epsilon)^2$.*

Proof. From Corollary 3.26, we know

$$\mathbb{P}((X_{n+1}, Y_{n+1}) \in \Gamma_{n,A}^\epsilon(D_1) \cap \Gamma_{n,A}^\epsilon(D_2)) \geq (1 - \epsilon)^2.$$

Thus,

$$\begin{aligned} \mathbb{P}(p_{\cap} \leq \epsilon) &= \mathbb{P}((\Gamma_{n,A}^\epsilon(D_1), \Gamma_{n,A}^\epsilon(D_2))^c) \\ &= 1 - \mathbb{P}(\Gamma_{n,A}^\epsilon(D_1), \Gamma_{n,A}^\epsilon(D_2)) \leq 1 - (1 - \epsilon)^2 \end{aligned}$$

From, the empirical approximation, Theorem 3.27, the probability of observing $p_{\cap} \leq \epsilon$ is then asymptotically bounded by $1 - (1 - \epsilon)^2$. \square

The main theoretical result of this paper summarizes the observations in this section as follows. Note that to make the statement precise we need to move from the statement about effectiveness at a point to a probabilistic statement. The most straightforward approach considers the ratio at a point, to a probabilistic statement, and for this we can take the expectation of the indicator for the set of (x, y) at which the attack is effective.

We summarize the above in the following theorem.

Theorem 3.39. *Suppose that D, P are samples from $(\mathcal{X} \times \mathcal{Y})^{n+1}$, that D is exchangeable, and that P is an effectively poisoned dataset with respect to D . Then D, P are conformally $(\epsilon, \epsilon, (1 - \epsilon)^2)$ -separable.*

4 Experimental Results

We cover experimental results in this section. Overall our goal is to demonstrate three points. First, that our empirical false negative (FNR) and false positive rates (FPR) are competitive with the state of the art in proactive defense provided by recent work [6]. Second, that our false negative rate is better

Task @ Poison Rate	Missed Detections (FNR)(%)	False Alarms (FPR) (%)	Poison Success Rate (%)
Patch GTSRB (SOA)	0.2	0.4	99.98
Patch GTSRB (Ours)	1.4	0.0	
Patch CIFAR (SOA)	1.7	1.8	100
Patch CIFAR (Ours)	1.2	1.6	
Witches’ Brew (Ours)	9.0	3.0	35

Table 1: Our separability analysis provides competitive detection rates against other proactive defenses. We also can detect the Witches’ Brew attack well.

than the theoretical bound and that our false positive rate is low. Third, to correct an *en passant* claim made by [3]. In this paper they claim that so-called label flipping and watermarking attacks (wherein the attacker only changes labels or superimposes a target onto images) can be detected by an application of “supervision”. They point to generic work that applies conformal prediction by throwing away any inferences that are not conformal at every layer of a neural network. However, neither a direct connection to detecting poison by non-conformity nor any claim that there is a valid test for poison is made. Second, they suggest that clean-label attacks using a bi-level optimization cannot be detected by supervision. Our experimental results can be used to show that one can indeed detect such “weak attacks” by conformal supervision. Moreover, we show that clean-label attacks can also be detected. In particular, we demonstrate that the gradient-matching “Witches’ Brew” attack can be detected using Conformal Separability. We summarize results comparing to state-of-the-art in Table 1. A detailed analysis of these individual results is given below.

Experimental Setup In order to compare with prior literature, we are using the CIFAR10 and GTSRB datasets. We start by training a WideResNet 28×10 model, and a three layer simple CNN for each dataset respectively from scratch and initialize the weights via He initialization [54]. We then create patches with size matching the filter size of the first layer of the model architecture to train it to kill that filter following the method discussed in [4]. Random samples are then poisoned with the patch in each epoch based on the pre-specified poison rates for 200 and 100 epochs. This process was carried out for both of the datasets. The position of the patch does not necessarily have to be fixed. Figure 5 shows sample CIFAR10 and GTSRB images with the patches applied. Note that the images are resized by about $7 \times$ for visualization purposes. However, the model is trained with much smaller images (32×32) and patches (7×7). For the optimization, we use the Adam optimizer with weight decays and learning rate schedulers. We use the cross-entropy loss function.

Evaluation Metrics Because we are interested in attacks that satisfy the *effectiveness* requirement of our proposed framework, we first look at *attack*



Figure 5: Sample CIFAR10 (top) and GTSRB (bottom) images with the patch applied.

success rates. The notion of success rate of an attack comes with some nuance. For the current paper, we simply define the success rate at S as the accuracy on a set of the form $\{(t_x, t_y) \mid (x, y) \in S\}$. This, e.g., grossly over approximates the success rate since it does not take into account cases where $t_y = y$ nor the rate at which the clean model guesses t_y ; however, it does seem to be the most common in the literature.

For evaluating our proposed Conformal Separability framework, we look at both false negative and false positive rates. While we know by Theorem 3.39 that we can bound the false negative rate of detecting poison, it is worth investigating the false positive rates. Additionally, *attack optimality* is evaluated. The attacks we are interested in do not always push towards optima on the poison rate spectrum. I.e., such attacks need not minimize imperceptibility (cf. Definition 3.11). This more relaxed position opens the door to a new question: if poison is not administered at an optimal dose, can we detect “enough” poison to render the attack inert? Our analyses reveal an enticing point on this front. It seems that when poison is applied at either too low or too high a rate the attack will not succeed. This suggests that there is a limited window of poison rates that yield effective attacks. However, this introduces a hitherto unexplored question: what is the maximum poison rate that we can make inert? Of course, due to our validity guarantee, we can always remove enough poison, but at what cost? We will demonstrate bounds on the *rates of poison* we can deal with.

4.1 Results on CIFAR10 and GTSRB

We now consider our results in connection with the patch-based poison attack summarized above on the CIFAR10 and GTSRB datasets. Table 2 displays the relationship between poison rate, the accuracy of the model on clean data and

DATASET	POISON RATE (%)	EVAL CLEAN (%)	SUCCESS RATE (%)
CIFAR10	0.0	93.35	10.0
CIFAR10	0.002	93.57	68.95
CIFAR10	0.01	93.35	97.57
CIFAR10	0.1	94.08	99.81
CIFAR10	0.2	94.01	100.00
CIFAR10	1	93.28	100.00
GTSRB	0.0	97.43	1.02
GTSRB	0.002	97.65	1.54
GTSRB	0.01	96.79	87.77
GTSRB	0.1	97.78	99.57
GTSRB	0.2	97.34	99.44
GTSRB	1	97.92	99.98

Table 2: Test accuracy (%) of a Wide ResNet 28×10 , and simple 3-layer CNN models trained from scratch respectively using clean and poisoned CIFAR10 and GTSRB data at multiple poison rates. Eval clean shows that the model maintains the same performance on clean data. Success rate shows that the attack becomes progressively more pronounced as the poison rate increases, taking a drastic leap in effectiveness from 0.002% to 0.01%. The orange rows indicate the poison rates prior to the “phase transition” from ineffective to effective attacks.

the success rate of the attack on poisoned data. The first column provides the rate at which we altered data in the training dataset. The second column shows that the attack does not alter validation accuracy of the trained model on the canonical CIFAR10 or GTSRB test set. The final column shows the success rate of the attack on CIFAR10 and GTSRB test set, and demonstrates that attack rate has a breadth of successful deployment rates.

To use Conformal Separability, we must identify a nonconformity score. Previous work on applying conformal prediction to neural networks ([41], [45]) used

$$A(D, x, y) = -s_{x,y} \quad \text{or} \quad A(D, x, y) = -\frac{\max_{j \neq y} s_{x,j}}{s_{x,y} + \gamma},$$

where we write $s_{x,y} := \text{softmax}(M_D(x))_y$ and γ is a parameter used to adjust the sensitivity to the y^{th} output [44]. These scores tended to produce slightly less confident predictions, due to uniformly noisy, non-dominant outputs. Also, the “tuning” parameter γ becomes a sort of hyperparameter of the conformal prediction, which we want to avoid. Yet such noise is captured well by entropy. Based on this observation, we consider more uniform distributions on the logits as “less conformal”, and indeed such distributions will have higher entropy. We then take as our non-conformity score, the entropy on the logits, relative to the self-information on the output in question. Explicitly, the non-conformity score

we use is:

$$A(D, x, y) = -\frac{\text{entropy}(\text{softmax}(M_D(x)))}{s_{x,y} \cdot \ln(s_{x,y})}.$$

Letting T be the training set and $P = T_C \uplus t_l(T_P)$ be the poisoned set, we apply Conformal Separability to T and P against a test set.

Recall that we derived a test for poison based on the Conformal Separability Test, where we can confidently claim that a test item x is poisoned when the measure of $\Gamma^\epsilon(T, x) \cap \Gamma^\epsilon(T_r, x)$ where T denotes a set of training data that is known to be clean and T_r denotes T with the poison applied at rate r . For evaluation, we choose hold-out sets of 500 poisoned and 500 clean items (x, y) that were never seen in training. We then use the Conformal Separability Test, evaluated over a range of poison rates r , to evaluate the intersections $\Gamma^\epsilon(T, x) \cap \Gamma^\epsilon(T_r, x)$. A *positive* identification of a purported poisoned item occurs when this intersection is empty and a *negative* when it is non-empty. Thus, a false positive occurs when a clean held-out sample x is identified as a positive and a false negative occurs when a poisoned held-out sample x is deemed a negative. The resulting false negative and positive rates at various conformal thresholds ϵ and poison rates are recorded in Table 3. As expected, false negative rates decrease dramatically as soon as the poison rate has increased to a sufficient level to yield an effective attack. Interestingly, in the case of CIFAR10, 9.8% of the poisoned items are correctly identified even when $r = 0$ so that $T_r = T$. I.e., $\Gamma^\epsilon(T, x) = \emptyset$ for 9.8% of the poisoned items x from the CIFAR10 hold-out set.

4.2 Witches-brew attack on CIFAR10

One advantage of the Conformal Separability Test (Algorithm 1) is that it opens the door to detection of attacks that might be too subtle in their manipulation of the training data to be readily detected. We experimented with one such example, the Witches Brew attack [3], that poisons a dataset to alter the classification of a fixed single target image x_t by making very small adjustments to a few (other) images. That is, it can be regarded as a kind of “distributed” version of an evasion attack in which the distribution is shifted by small perturbation of several images in order to yield misclassification of the target image. In general, the target image itself will not be manipulated in this attack. The attack parameters are the poison rate, attack distance, and attack size. The poison rate is as defined above. Another parameter of the the attack is the attack distance $\delta > 0$ which provides a bound on the total amount of change that each image can undergo (the attack stays with in a ball of radius δ centered on the image being manipulated). The attack size provides a budget for the number of pixels that can be manipulated. After setting these parameters, there are five ingredients provided to the attack, as depicted in Figure 6. The target image x_t can be an image from any class. The *intended class* is the class that we want the model to assign to x_t . For example, given an image x_t of a Labrador retriever and the intended class, “sea lion”, the attack aims to cause x_t to be classified as “sea lion.” The *poison class* is the class from which images

DATASET	POISON RATE (%)	FALSE NEGATIVE RATE (%)			FALSE POSITIVE RATE (%)		
		Conformal Threshold			Conformal Threshold		
		0.1	0.05	0.01	0.1	0.05	0.01
CIFAR10	0.0	90.2	90.2	90.2	0.0	0.0	0.0
CIFAR10	0.002	47.8	48.0	48.8	0.4	0.4	0.4
CIFAR10	0.01	6.2	6.4	6.6	0.0	0.0	0.0
CIFAR10	0.1	2.2	2.4	2.4	0.8	0.8	0.8
CIFAR10	0.2	1.2	1.4	1.4	1.0	1.0	1.0
CIFAR10	1.0	1.2	1.4	1.4	1.6	1.6	1.6
GTSRB	0.0	100	100	100	0.0	0.0	0.0
GTSRB	0.002	99.5	99.7	100	0.16	0.16	0.0
GTSRB	0.01	27.1	27.5	43.8	0.16	0.16	0.0
GTSRB	0.1	2.2	2.3	14.1	0.0	0.0	0.0
GTSRB	0.2	3.3	3.5	15.4	0.0	0.0	0.0
GTSRB	1.0	1.4	1.7	14.3	0.0	0.0	0.0

Table 3: Evaluation of FNR and FPR on CIFAR10 and GTSRB where the evaluation is carried out on held-out poisoned and clean samples x (each of size 500). Following the Conformal Separability Test, the intersection $\Gamma^\epsilon(T, x) \cap \Gamma^\epsilon(T_r, x)$ is evaluated for each poison rate r and conformal threshold ϵ considered, where T is the respective training set and T_r is the result of poisoning T at rate r . Our FNRs for effective attacks come in lower than the theoretical bound established in Corollary 3.26. Indeed, the sharp drop in FNR is correlated with the increase in success rate from Table 2. Even for unsuccessful attacks, we catch some of the poisoned samples. Additionally, our false positive rate shows that our test does not throw out good data. The orange rows indicate the poison rates prior to the “phase transition” from ineffective to effective attacks.

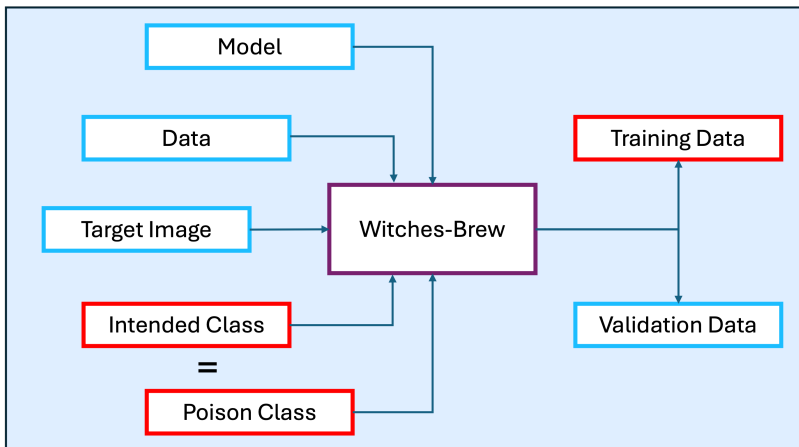


Figure 6: The Conformal Separability Test can be used to detect attacks that make very few changes to the training set. We experimented with and were able to detect the Witches’ Brew attack [3] which pushes a target image to be misclassified by a model trained on the poisoned data, but where the target image and its label are not manipulated in the training set. Shown here are the inputs and outputs of the attack.

will be poisoned. Note that the poison class need not be the actual class of the target image. In our experiments we only considered the case where the intended class and the poison class are identical, which was also the setting of the experiments reported in *ibid*.

Since the attack targets pre-selected images, we cannot simply apply the attack to additional test images after model training. Thus, this is an expensive attack to carry out. To analyze the success rate and detection capabilities of this attack, we train clean and poisoned model pairs 100 times, and test on attacked images. We fix a poison rate of 1.1%. The attack success rate over the 100 tests is 35%. With a conformal threshold of 0.15, we obtain a false negative rate of 9% thus reducing the attack effectiveness to 3.5%. The false positive rate is 3%. Thus, if we applied the mitigation to the data we would still have enough data to adequately train. Thus, we have demonstrated that it is possible to detect and mitigate even attacks that manipulate training data in such a way as to impact performance on *other* unmanipulated data. Such attacks are *a priori* harder to detect than common patch attacks.

5 Conclusion and Future work

In this paper we established that moving to a view of dataset poisoning as a stochastic problem captures poisoning attacks well. Indeed, we showed that the definition of a trigger attack can be formulated directly using notions from distribution-free statistics (Definitions 3.30,3.31,3.33). We provided theoretical

evidence (Theorem 3.39) that these definitions adequately capture the notion of poison. Indeed for datasets D_1, D_2 which may be different and may have different random errors in the models they produce, we showed that the statistical geometry of their conformal prediction sets determines poison with provably bounded error on missed detection. Moreover, we made no assumptions on the function guiding the attack meaning that this bounded detection rate works, for example, even against adversaries that create poisons using Turing-undecidable functions. We also provided experimental evidence that this test does not capture superfluous information that causes the geometry to capture too much more than the poisoned items by showing experimentally low false positive rates (Section 4). We also demonstrated experimentally that even subtle “clean-label” attacks do admit a computationally effective test. Finally, our theoretical and experimental results provide a sound foundation for practical security against attacks in a scenario where the goal is to preserve the integrity of a clean set of training data (the so-called proactive safety goal).

On the theoretical side, we showed that no poisoned item can be exchangeable with a clean distribution of data. However, we did not rule out that no poisoned item can be identically distributed. Indeed one way to obtain this might be to craft a poison which acts, for all intents and purposes as a singularity in the distribution, so that the surface of poisoned items has measure zero. For certain neural network models and activation functions, it is not entirely clear that this is possible. One way to achieve this would be to have a catastrophic surface that produces a cusp around a poisoned item, which, upon projection in a future layer shows up as a proper singularity (to within floating point arithmetic). Another possibility would be to construct clean label attacks that are identically distributed; for example an attack like [2]. One could imagine crafting such a scenario that forces all items in a dataset to be in-distribution, but where the order and frequency are amiss (hence breaking a symmetry invariance). It would certainly be interesting to know conditions that permit identically distributed poisons.

On the theoretical and practical sides, it would be interesting to directly model or explore the surface of the intersection of conformal prediction sets as a kind of statistical surface. In the label classification example, it would be interesting to know whether this surface must put a dynamics on the state space that pulls items absolutely close together. Given some assumptions on the distribution, for example, Lipschitz, it may be possible to then further our result and derive a provable guarantee for detection methods for a class of poisons which rely on distance (e.g. a k-nearest-neighbors test) in some latent space. This could also then provide a way to bootstrap the test with even less clean data, and for some classes of poison, possibly with no clean data required to boot.

We showed that having access to some clean data allows us to develop a practical test for poison and is immediately applicable to proactively protecting datasets. What we do not currently know is any kind of lower bound on the amount of clean data required. It would be theoretically interesting if there is some class of poison attacks which provably require *some* clean data to detect;

it would also be interesting to relate the amount of clean data required to some kind of complexity measure of the model.

One curiosity we discovered in performing our experiments is that often the relationship between poison-rate and poison effectiveness is sharp. For example, for both the GTSRB and CIFAR datasets, there seems to be almost a phase transition in how a small amount of increase in poison-rate affects the success rate (see Table 2) at around a 0.002 poison rate. To our knowledge, there has been no analysis of phase transitions in the study of dataset poisoning, and it would be interesting to know when there can be no constant bounding the relationship of poison-rate to success-rate.

References

- [1] T. Gu, B. Dolan-Gavitt, and S. Garg, “Badnets: Identifying vulnerabilities in the machine learning model supply chain,” *arXiv preprint arXiv:1708.06733*, 2017.
- [2] A. Shafahi, W. R. Huang, M. Najibi, *et al.*, “Poison frogs! targeted clean-label poisoning attacks on neural networks,” *Advances in neural information processing systems*, vol. 31, 2018.
- [3] J. Geiping, L. Fowl, W. R. Huang, *et al.*, “Witches’ brew: Industrial scale data poisoning via gradient matching,” *arXiv preprint arXiv:2009.02276*, 2020.
- [4] A. Khaddaj, G. Leclerc, A. Makelov, *et al.*, “Rethinking backdoor attacks,” in *International Conference on Machine Learning*, PMLR, 2023, pp. 16 216–16 236.
- [5] A. Schwarzschild, M. Goldblum, A. Gupta, J. P. Dickerson, and T. Goldstein, “Just how toxic is data poisoning? a unified benchmark for backdoor and data poisoning attacks,” in *International Conference on Machine Learning*, PMLR, 2021, pp. 9389–9398.
- [6] X. Qi, T. Xie, J. T. Wang, T. Wu, S. Mahloujifar, and P. Mittal, “Towards a proactive ml approach for detecting backdoor poison samples,” in *Usenix Security*, vol. 32, 2023, pp. 1685–1702.
- [7] C. Sun, A. Shrivastava, S. Singh, and A. Gupta, “Revisiting unreasonable effectiveness of data in deep learning era,” in *Proceedings of the IEEE international conference on computer vision*, 2017, pp. 843–852.
- [8] J. Cho, K. Lee, E. Shin, G. Choy, and S. Do, “How much data is needed to train a medical image deep learning system to achieve necessary high accuracy?” *arXiv preprint arXiv:1511.06348*, 2015.
- [9] A. Munappy, J. Bosch, H. H. Olsson, A. Arpteg, and B. Brinne, “Data management challenges for deep learning,” in *2019 45th Euromicro Conference on Software Engineering and Advanced Applications (SEAA)*, IEEE, 2019, pp. 140–147.

- [10] T. Rocktäschel and S. Riedel, “Learning knowledge base inference with neural theorem provers,” in *Proceedings of the 5th workshop on automated knowledge base construction*, 2016, pp. 45–50.
- [11] X. Chen, C. Liu, B. Li, K. Lu, and D. Song, “Targeted backdoor attacks on deep learning systems using data poisoning,” *arXiv preprint arXiv:1712.05526*, 2017.
- [12] L. Muñoz-González, B. Biggio, A. Demontis, *et al.*, “Towards poisoning of deep learning algorithms with back-gradient optimization,” in *Proceedings of the 10th ACM workshop on artificial intelligence and security*, 2017, pp. 27–38.
- [13] J. Deng, W. Dong, R. Socher, L.-J. Li, K. Li, and L. Fei-Fei, “ImageNet: A Large-Scale Hierarchical Image Database,” in *CVPR09*, 2009.
- [14] Y. Zeng, W. Park, Z. M. Mao, and R. Jia, “Rethinking the backdoor attacks’ triggers: A frequency perspective,” in *Proceedings of the IEEE/CVF international conference on computer vision*, 2021, pp. 16 473–16 481.
- [15] M. Goldblum, D. Tsipras, C. Xie, *et al.*, “Dataset security for machine learning: Data poisoning, backdoor attacks, and defenses,” *IEEE Transactions on Pattern Analysis and Machine Intelligence*, vol. 45, no. 2, pp. 1563–1580, 2022.
- [16] A. Madry, A. Makelov, L. Schmidt, D. Tsipras, and A. Vladu, “Towards deep learning models resistant to adversarial attacks,” *arXiv preprint arXiv:1706.06083*, 2017.
- [17] S. Huang, N. Papernot, I. Goodfellow, Y. Duan, and P. Abbeel, “Adversarial attacks on neural network policies,” *arXiv preprint arXiv:1702.02284*, 2017.
- [18] A. Turner, D. Tsipras, and A. Madry, “Clean-label backdoor attacks,” 2018.
- [19] R. T. Mercuri and P. G. Neumann, “Security by obscurity,” *Communications of the ACM*, vol. 46, no. 11, p. 160, 2003.
- [20] S. Kumar, *How wikipedia is served to you: A complex web of open source and caching*.
- [21] H. Huang, Z. Zhao, M. Backes, Y. Shen, and Y. Zhang, “Composite backdoor attacks against large language models,” *arXiv preprint arXiv:2310.07676*, 2023.
- [22] P. V. Falade, “Decoding the threat landscape: Chatgpt, fraudgpt, and wormgpt in social engineering attacks,” *arXiv preprint arXiv:2310.05595*, 2023.
- [23] K. Afifi-Sabet, *Poisoned ai went rogue during training and couldn’t be taught to behave again in ‘legitimately scary’ study*, Article: <https://www.livescience.com>, Jan. 2024.
- [24] Z. Xie, J. Brophy, A. Noack, *et al.*, “Identifying adversarial attacks on text classifiers,” *arXiv preprint arXiv:2201.08555*, 2022.

- [25] ryanrudes, *Wikimedia-commons-dataset*.
- [26] N. Carlini, M. Jagielski, C. A. Choquette-Choo, *et al.*, “Poisoning web-scale training datasets is practical,” *arXiv preprint arXiv:2302.10149*, 2023.
- [27] T. Thomson, *Data poisoning: How artists are sabotaging ai to take revenge on image generators*, <https://theconversation.com/data-poisoning-how-artists-are-sabotaging-ai-to-take-revenge-on-image-generators-219335>, Dec. 2023.
- [28] K. Maag and A. Fischer, “Uncertainty-weighted loss functions for improved adversarial attacks on semantic segmentation,” in *Proceedings of the IEEE/CVF Winter Conference on Applications of Computer Vision*, 2024, pp. 3906–3914.
- [29] P. Ratanaworabhan, V. B. Livshits, and B. G. Zorn, “Nozzle: A defense against heap-spraying code injection attacks,” in *USENIX security symposium*, 2009, pp. 169–186.
- [30] M. Jagielski, G. Severi, N. Pousette Harger, and A. Oprea, “Subpopulation data poisoning attacks,” in *Proceedings of the 2021 ACM SIGSAC Conference on Computer and Communications Security*, 2021, pp. 3104–3122.
- [31] OECD, “Ai language models: Technological, socio-economic and policy considerations,” *OECD*, vol. 352, p. 1, 2023.
- [32] J. Zhang and D. Tenney, “The evolution of integrated advance persistent threat and its defense solutions: A literature review,” *Open Journal of Business and Management*, vol. 12, no. 1, pp. 293–338, 2023.
- [33] Ł. Korycki and B. Krawczyk, “Adversarial concept drift detection under poisoning attacks for robust data stream mining,” *Machine Learning*, vol. 112, no. 10, pp. 4013–4048, 2023.
- [34] N. Peri, N. Gupta, W. R. Huang, *et al.*, “Deep k-nn defense against clean-label data poisoning attacks,” in *Computer Vision–ECCV 2020 Workshops: Glasgow, UK, August 23–28, 2020, Proceedings, Part I 16*, Springer, 2020, pp. 55–70.
- [35] N. Müller, D. Kowatsch, and K. Böttinger, “Data poisoning attacks on regression learning and corresponding defenses,” in *2020 IEEE 25th Pacific Rim International Symposium on Dependable Computing (PRDC)*, IEEE, 2020, pp. 80–89.
- [36] T. Zhao, Y. Liu, L. Neves, O. Woodford, M. Jiang, and N. Shah, “Data augmentation for graph neural networks,” in *Proceedings of the aaai conference on artificial intelligence*, vol. 35, 2021, pp. 11 015–11 023.
- [37] Y. Ma, X. Zhu, and J. Hsu, “Data poisoning against differentially-private learners: Attacks and defenses,” *arXiv preprint arXiv:1903.09860*, 2019.

- [38] M. Abadi, A. Chu, I. Goodfellow, *et al.*, “Deep learning with differential privacy,” in *Proceedings of the 2016 ACM SIGSAC conference on computer and communications security*, 2016, pp. 308–318.
- [39] A. Khaddaj, G. Leclerc, A. Makelov, *et al.*, “Backdoor or feature? a new perspective on data poisoning,”
- [40] M. Xue, C. Yuan, H. Wu, Y. Zhang, and W. Liu, “Machine learning security: Threats, countermeasures, and evaluations,” *IEEE Access*, vol. 8, pp. 74 720–74 742, 2020.
- [41] V. Vovk, A. Gammerman, and G. Shafer, *Algorithmic Learning in a Random World*. Springer, 2022, ISBN: 9783031066481.
- [42] A. Gammerman, V. Vovk, and V. Vapnik, “Learning by transduction,” *Uncertainty in Artificial Intelligence*, vol. 14, pp. 148–155, 1998.
- [43] R. Laxhammar, “Conformal anomaly detection,” Ph.D. dissertation, University of Skövde, 2014.
- [44] H. Papadopoulos, V. Vovk, and A. Gammerman, “Conformal prediction with neural networks,” in *19th IEEE International Conference on Tools with Artificial Intelligence (ICTAI 2007)*, vol. 2, 2007, pp. 388–395. DOI: [10.1109/ICTAI.2007.47](https://doi.org/10.1109/ICTAI.2007.47).
- [45] V. Balasubramanian, S.-S. Ho, and V. Vovk, *Conformal Prediction for Reliable Machine Learning*. Morgan Kaufmann, 2014, ISBN: 9780123985378.
- [46] G. Shafer and V. Vovk, “A tutorial on conformal prediction.,” *Journal of Machine Learning Research*, vol. 9, no. 3, 2008.
- [47] C. Saunders, A. Gammerman, and V. Vovk, “Transduction with confidence and credibility,” in *Sixteenth International Joint Conference on Artificial Intelligence (IJCAI 99)*, 1999, pp. 722–726.
- [48] R. J. Tibshirani, R. Foygel Barber, E. Candes, and A. Ramdas, “Conformal prediction under covariate shift,” in *Advances in Neural Information Processing Systems*, H. Wallach, H. Larochelle, A. Beygelzimer, F. d’Alché-Buc, E. Fox, and R. Garnett, Eds., vol. 32, Curran Associates, Inc., 2019.
- [49] E. Çinlar, *Probability and Stochastics* (Graduate Texts in Mathematics). Springer, 2011.
- [50] V. Glivenko, “Sulla determinazione empirica delle leggi di probabilità,” *Giornale dell’Istituto Italiano degli Atturai*, vol. 4, pp. 92–99, 1933.
- [51] F. Cantelli, “Sulla determinazione empirica delle leggi di probabilità,” *Giornale dell’Istituto Italiano degli Atturai*, vol. 4, pp. 421–424, 1933.
- [52] B. De Finetti, “Sull’ Approssimazione empirica di una legge di probabilità,” *Giornale dell’Istituto Italiano degli Atturai*, vol. 4, no. 3, pp. 415–420, 1933.
- [53] A. Dvoretzky, J. Kiefer, and J. Wolfowitz, “Asymptotic minimax character of the sample distribution function and of the classical multinomial estimator.,” *Annals of Mathematical Statistics*, 2956.

- [54] K. He, X. Zhang, S. Ren, and J. Sun, “Delving deep into rectifiers: Surpassing human-level performance on imagenet classification,” in *Proceedings of the IEEE international conference on computer vision*, 2015, pp. 1026–1034.